Chapter 5

Blending of polymer with fumed silica as a filler

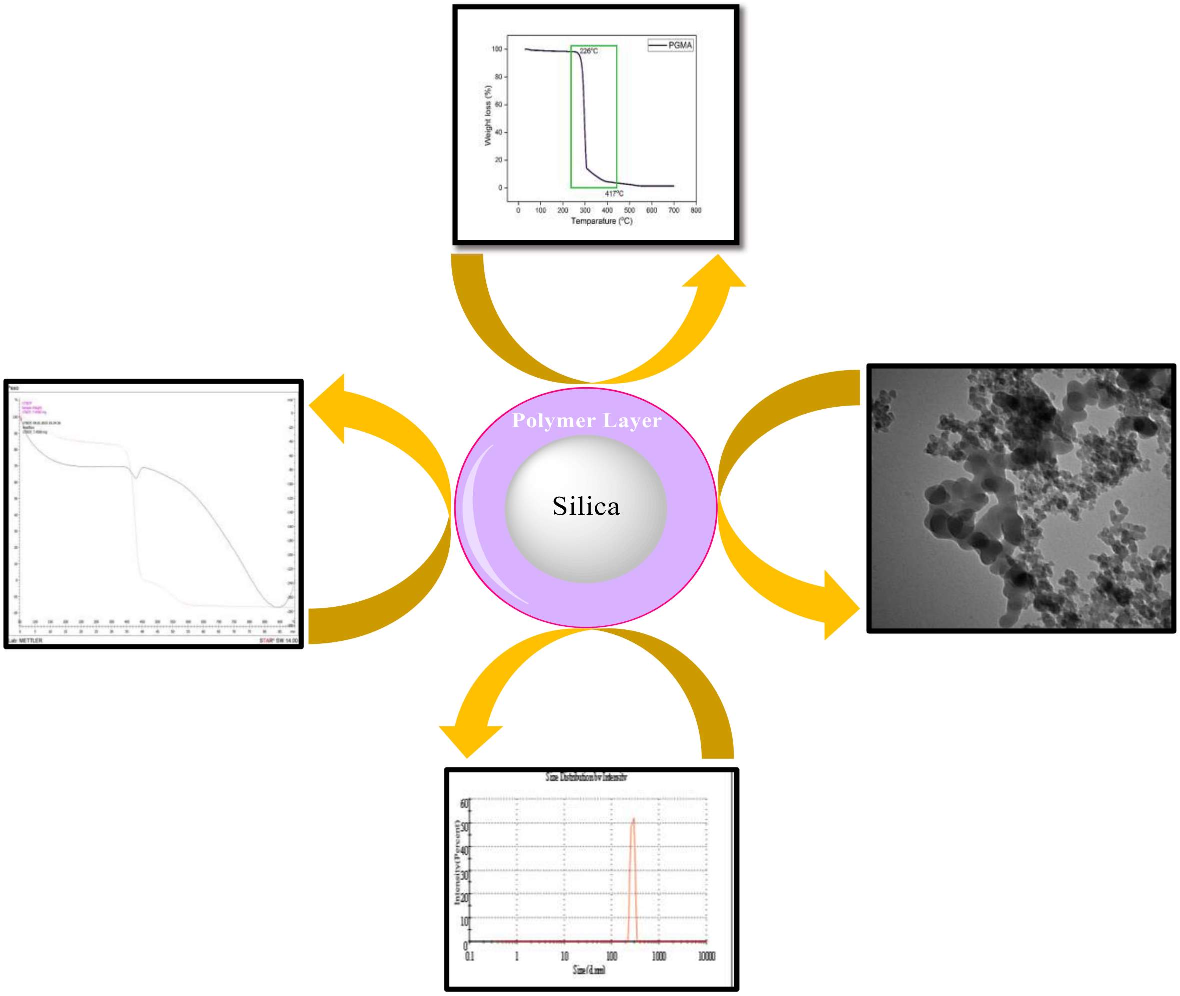

5.1. Introduction

The inclusion of well-defined organic and inorganic components into a single material is one of the methods to synthesize nanocomposites. The addition of well-defined polymers into inorganic substrates are extremely significant as the functionality, structure, and dimensions of these macromolecules allow the incorporation of specific characteristic into the resulting hybrid material.

The introduction of fumed silica is previously explained in chapter 1 of this thesis, whereas the present chapter summarizes the synthesis of PMMA via ATRP technique[8, 9] , and its comparative study with the grafted polymer, SiO_2-g-PMMA. In this work, the brominated fumed silica as a macro initiator is used to prepare SiO_2-g-PMMA, and SiO_2-g-PGMA grafted polymers. The synthesis of this brominated fumed silica was carried out by the purification of the fumed silica and its functionalization with Bromine (-Br) group[10–12], and then its grafting process was carried out by MMA as well as GMA monomer via ATRP. The synthesis of PMMA via ATRP was confirmed via FT-IR analysis, whereas the formation of SiO_2-g-PMMA, and SiO_2-g-PGMA were confirmed by FT-IR and EDS analysis. The information of surface morphology and its particle size was given by the TEM analysis. Moreover, the DLS analysis confirmed that after monomer attachment, and on increasing the functionalization of bromine, the particle size of the silica grafted material was increased, and the percentage weight loss of the grafted polymers obtained from TGA analysis was used to calculate percentage grafting (%G) was calculated using the results of TGA[13, 14] analysis of SiO_2-g-PMMA[6, 15], and SiO_2-g-PGMA[16, 17].

The synthesis of grafted fumed silica through different monomer was already done by other researchers [give examples and references]. The novelty of this work is to be performed with the fumed silica having particle size is 151.7 nm by DLS analysis. Furthermore, these grafted fumed silica with polymeric layers of PMMA, and PGMA respectively were blended with the synthesized polymer (PS-*b*-PDMS-*b*-PS) its detailed description is given in chapter 3, where fumed silica acted as filler. The blending capacity, and thermal stability of prepared blends were investigated via TGA analysis.

5.2. Materials and Methods

Fumed Silica (Fumed SiO_2) Aerosil 200 was purchased from Evonik; Acetone (Loba Chemie, 99%); n-Hexane (Loba Chemie, 99%); Toluene (Loba Chemie, 99.5%); $CHCl_3$ (Loba Chemie, 99.8%); THF (Tetrahydrofuran) (Loba Chemie, 99.8%); Methanol (Loba Chemie, 99.8%); HCl (Loba Chemie, 35%)**;** Ethanol (Loba Chemie, 97%)**;** Glacial Acetic Acid (Loba Chemie, 99.7%)**;** α- BIBB (Aldrich, 98%); CuCl (Aldrich, 97%), CuBr (Aldrich, 99.99%) were purified by washing with glacial acetic acid, ethanol and acetone before use; Bpy (Aldrich, >99%); PMDETA (Aldrich, 99%); MMA (Aldrich, 99%); GMA (Aldrich, 97%) both were passed through activated basic and neutral alumina to remove inhibitors, subsequently dried over molecular sieve for 24 h before use; DMDBHD (Aldrich, 97%).

ALPHA (Bruker optics Inc, Germany) Fourier transform infrared spectroscopy (FT-TR) study at 28°C. All the compounds were scanned with a KBr pellet over a wavelength range of 4000-400 cm^{-1}. The elemental investigations were conducted using an EDS analysis using a JEOL JSM-5610LV Scanning Electron Microscope from Akishima in Tokyo, Japan. Agilent Technologies' gel permeation chromatography (GPC) is used to measure the Mn, Mw and PDI, with all samples taken at 1 mg and dissolved in HPLC grade tetrahydrofuran (THF). Thermal stability was assessed using the Exstar (Stage II TG/DTA-6300) TGA instrument. The particle size was determined using the Zetasizer ZS90 (Malvern Instruments, Worcester, UK). For the analysis, a 5 Mw He-Ne laser (632.8 nm) operating at 25°C with a scattering angle of 90° was used.

5.3. Experimental Section

5.3.1. Preparation of PMMA via ATRP

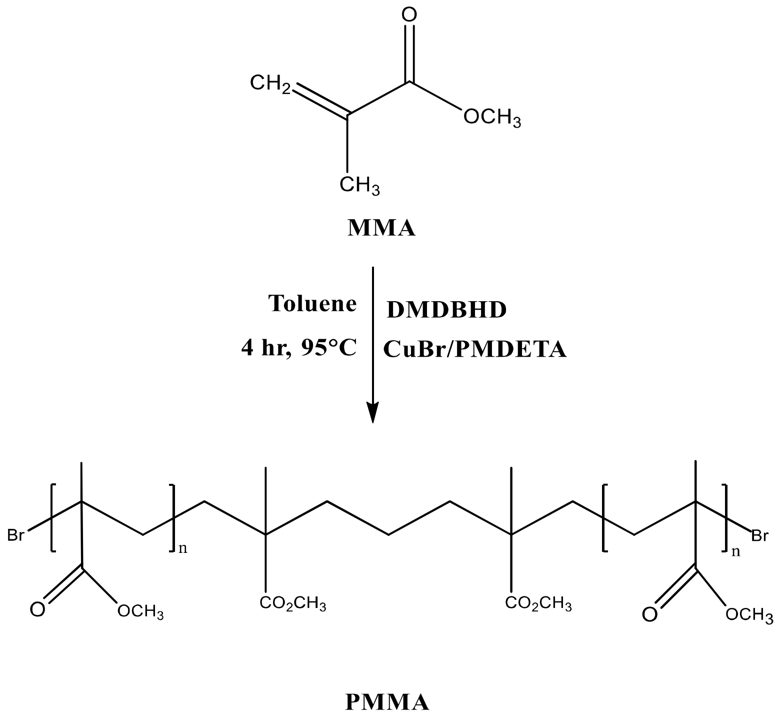

Scheme 4. Preparation of PMMA via ATRP.

Initially, purified CuBr (0.02g, 0.141 mmol) and wash were first placed in a 20 mL vial with a magnetic stirrer bar and sealed with a rubber septum while being immersed in a stream of flowing Argon. Deoxygenated PMDETA (0.048g, 0.282 mmol) in MMA (3 mL) was added to this using a cannula tube. DMDBHD (0.04g, 0.14 mmol) and 5 mL of toluene as a solvent were added to the mentioned vial, and the mixture was mixed well before the temperature was gradually raised to 95 °C.

Purification of Reaction Mixture

The reaction was terminated by air exposure and the reaction was diluted with 50 mL of THF. To remove the catalyst ligand combination from this reaction mixture, it was passed through an activated neutral alumina column. The polymer was precipitated out with large volume of methanol, the product was dried and purified three times in this manner.

$$\% \text{ Conversion} = \text{yield} / \text{total quantity of monomer} * 100$$

$$= 0.5 \text{ g}/2.82 \text{ g} * 100 = 17.73 \%$$

$$M_n \text{ (Theoretical)} = I + \text{M.W of Monomer}/I * \text{Conversion}$$

$$= 346 + 200/1 * 0.1773$$

$$M_n \text{ theoritical} = 3892 \text{ g/mol}$$

$$M_n \text{ GPC} = 3138 \text{ g/mol}$$

Fig 5.1. (A) Experimental Setup of ATRP Synthesis (B) Product of ATRP (PMMA).

5.3.2. Activation of Silone group

Fumed silica Aerosil 200 was purchased from M/s Evonik which was coated by oil (hydrocarbon). Furthermore, for the removal of this oil, coated fumed silica was taken (8.3g,) and which was poured in 500 mL mixture of n-hexane and acetone solvent. After thorough stirring, the silica was filtered and dried. 8.1g of purified fumed silica was obtained which was used for the further modification as well as grafting with polymer.

5.3.3. Surface Modification to Bromine Group

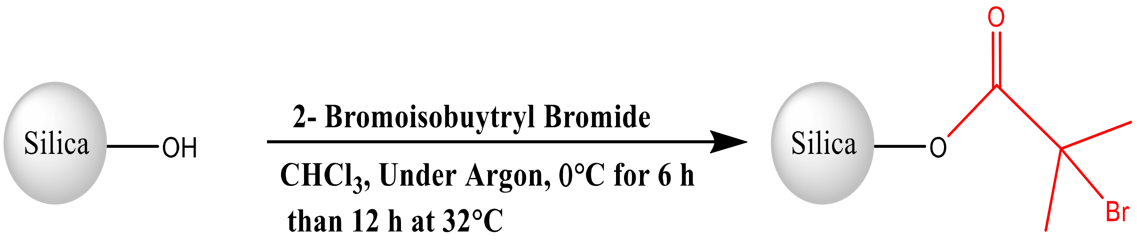

Si - OH **Si - Br**

Scheme 5. Surface modification to bromine (Br) group on the surface of fumed silica.

Experimental

Took 3.0g of purified silica and 50 mL of chloroform and combined them in a three-necked RBF. After three hours of sonication, the mixture was homogeneous, and the reaction mixture was bubbled with inert atmosphere of argon. Through an addition funnel, BIBB (2–3 mL) and chloroform (10 mL) were then added to the flask. To keep the temperature at 0°C for 6 hours, it was put in an ice bath. The reaction was then allowed at room temperature for 12 hours. Poured the reaction mixture in n-hexane (approx. 50 mL) and kept it to settle down for 2-3h. Then decanted the upper solution carefully and centrifuge the remaining reaction mixture at 2000 RPM. The reaction mixture was kept in an oven for 3h at 50°C until it was completely dry.

Fig 5.2 (A) Experimental Setup (B) Brominated Fumed Silica.

5.3.4. Preparation of Polymer Grafted Silica Using MMA as Monomer via ATRP

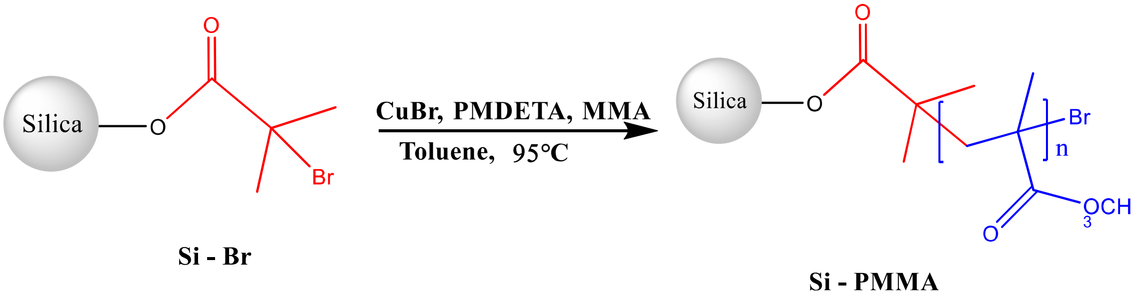

Scheme 6 ATRP Synthesis for the preparation of SiO_2-g-PMMA.

Experimental

Brominated fumed silica (0.3g, 0.6 mmol) was introduced to a vial together with CuCl (0.059g, 0.6 mmol) as the catalyst and Bpy (0.187g, 1.2 mmol) as the ligand. MMA monomer (19 mL, 180 mmol) was also added to the second vial along with 10 mL of toluene solvent. Argon was then used to purge the solution for five minutes. Through the cannula tube, the mixture from the second vial is added to the reaction mixture in the first vial. The resulting mixture was placed 24 hours in an oil bath at 95°C. After the polymerization, the reaction mixture was poured into THF, precipitated in methanol, and washed repeatedly with methanol to remove the unreacted materials. Additionally, 1-2 drops of strong HCl were also added to the methanol to remove the copper complex. The product was ultimately dried in an oven for 24 hours at 60°C. Weighing it when had fully dried and yielded of 0.1g.

Fig 5.3. (A) Experimental Setup of ATRP Synthesis (B) Product (SiO_2-g-PMMA).

5.3.5. Preparation of Polymer Grafted Silica Using GMA as Monomer via ATRP

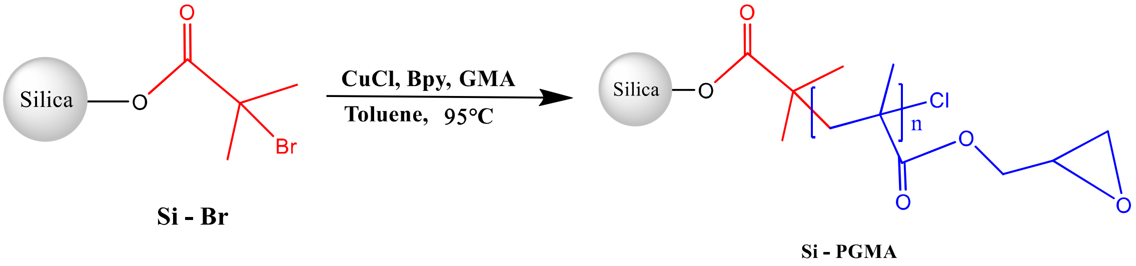

Scheme 7. ATRP Synthesis for the preparation of SiO_2-g-PGMA.

Experimental

In the experiment, a brominated fumed silica initiator (0.39g, 0.6 mmol) was added to a first round bottom flask (RBF) along with a copper chloride catalyst (0.059g, 0.6 mmol) and a bpy ligand (0.187g, 1.2 mmol). Next, a solution of GMA monomer (24.53 mL, 180 mmol) in toluene (10 mL) was added to a second RBF. The resulting solution was purged with argon for 5 minutes to create an inert atmosphere. The solution in the second RBF was then transferred to the first RBF through a cannula tube, effectively combining the two solutions. The resulting mixture was heated to 95℃ for 24 hours in an oil bath to initiate a radical polymerization reaction, whereby the initiator, catalyst, and ligand facilitated the polymerization of the GMA monomer. After the completion of polymerization, the reaction mixture was poured into THF and subsequently precipitated in methanol. The precipitated product was washed with methanol multiple times to remove any unreacted materials. Additionally, 1-2 drops of concentrated hydrochloric acid (conc. HCl) were added to the methanol to remove the copper complex. After washing, the product was dried in an oven at 60℃ for 24 hours until it was completely dry. Once dry, the final product was weighed, and the total yield was found to be 22.42g..

Fig 5.4 (A) Experimental setup of ATRP synthesis (B) product (SiO_2-g-PGMA).

5.3.6. Preparation of a film by blending of polymer with fumed silica as a filler

In Chapter 3, the synthesized triblock copolymer PS-b-PDMS-b-PS was used as a polymeric material with purified fumed silica as nanofillers to prepare three different films. To prepare each of the three films, a 23% dop solution was made using a total of 2 mL of $CDCl_3$ solvent. For the first film, 0.46 g of PS-*b*-PDMS-*b*-PS polymer was dissolved in the solvent. Then, 0.5% purified fumed silica (0.0023 g) was added and stirred constantly at 28℃ for 24 hours. The resulting dop solution was cast onto a clean glass plate using an applicator with a gap size of 200 µm. The plate was left in the air for 30 minutes as a dry phase inversion. In the second film, the dop solution was the same as in the first film, but the filler used was functionalized brominated silica. For the third film, SiO_2-g-PMMA was added as a filler. All films were successfully prepared using the above method and were used for further studies. The images of the prepared films are given below in Figure 5.5.

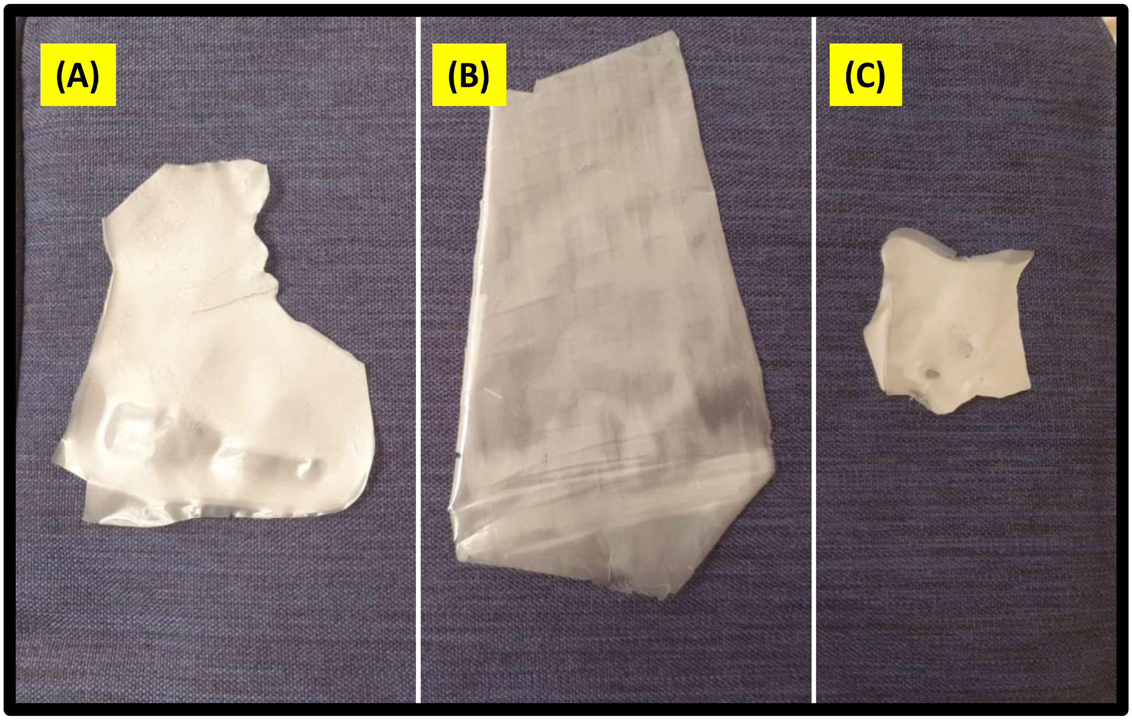

Figure 5.5. Images of polymer blend with nanofillers (A) Polymer with pristine fumed silica, (B) Polymers with functionalized fumed silica, (C) Polymer with grafting fumed silica.

5.4. Results and discussion

In Figure 5.6, ATR-FT-IR spectroscopy was performed to confirm the polymerization of MMA monomer to PMMA. The obtained spectrum showed distinct bands for different functional groups such as $–CH_2$, $-CH_3$, -C=O, and $-O-CH_3$ functional groups at 2954, 2850, 1732, and 1439 cm^{-1}, respectively. This data confirmed the successful polymerization of MMA through ATRP.

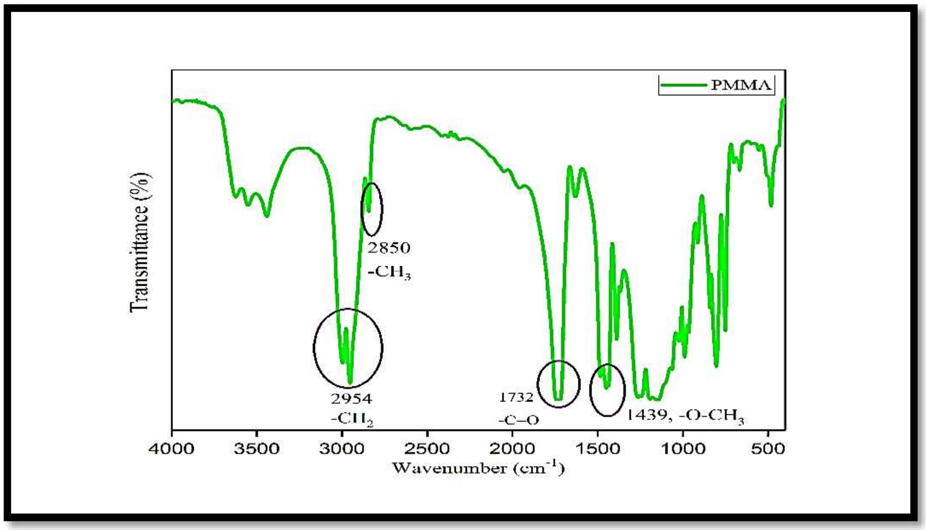

Figure 5.6 FT-IR Analysis of PMMA.

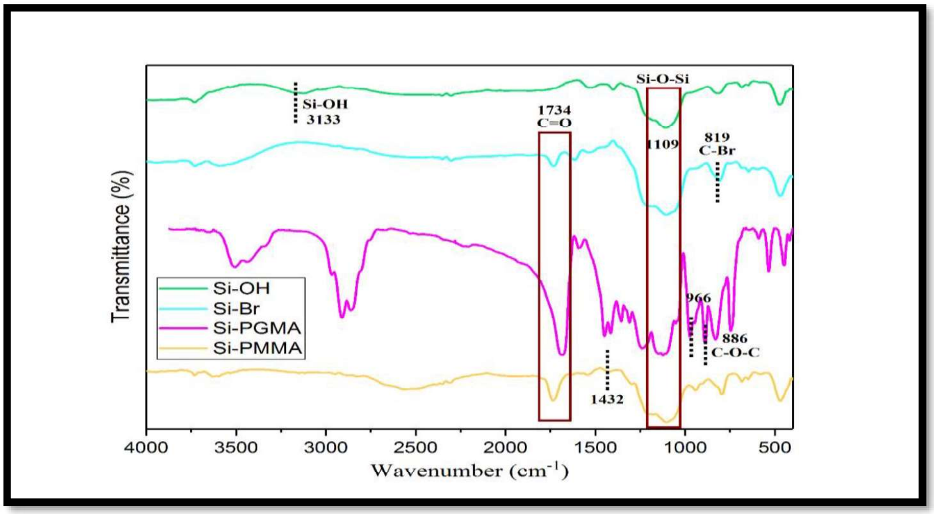

Figure 5.7 FT-IR Analysis of (A)Si-OH, (B)Si-Br, (C)Si-PMMA and (D)Si-PGMA.

ATR-FT-IR spectroscopy was performed to confirm the successful grafting of PMMA chains onto the silica nanoparticles, as demonstrated in Fig 5.7. The signal of Si-O-Si stretching at 1120 cm^{-1} was clearly observed in the spectrum of the purified silica. Following the bromination reaction, a C=O stretching peak near 1734 cm^{-1} was observed in the silica nanoparticles due to the carbonyl group of the macro initiator. In contrast, the spectrum of SiO_2-g-PMMA displayed additional CH_2 and CH_3 stretching modes in the range of 2954 cm^{-1} to 2850 cm^{-1}, which are also present in the spectra of pure PMMA. This finding indicates that the PMMA chains were successfully grafted onto the silica nanoparticles. Moreover, peaks resulting from bending vibrations of CH_2 at 1432 cm^{-1} and CH_3 at 1390 cm^{-1} were observed for SiO_2-g-PMMA. The intensity of the stretching at 1730 cm-1 increased after ATRP reaction, which can be attributed to the superposition of the carbonyl groups of the macro initiator and PMMA. The appearance of the absorption band at 1731 cm^{-1}, attributable to the carbonyl stretching vibration of the ester group of PGMA, confirmed the presence of SiO_2-g-PGMA. Additionally, absorption peaks at 966 cm^{-1} and 886 cm^{-1} were reasonably attributed to the epoxide groups of the surface-grafted PGMA. Thus, SiO_2-g-PGMA with a high density of epoxide groups is promising for applications in hybrid molecular-semiconductor devices or chemical biosensors.

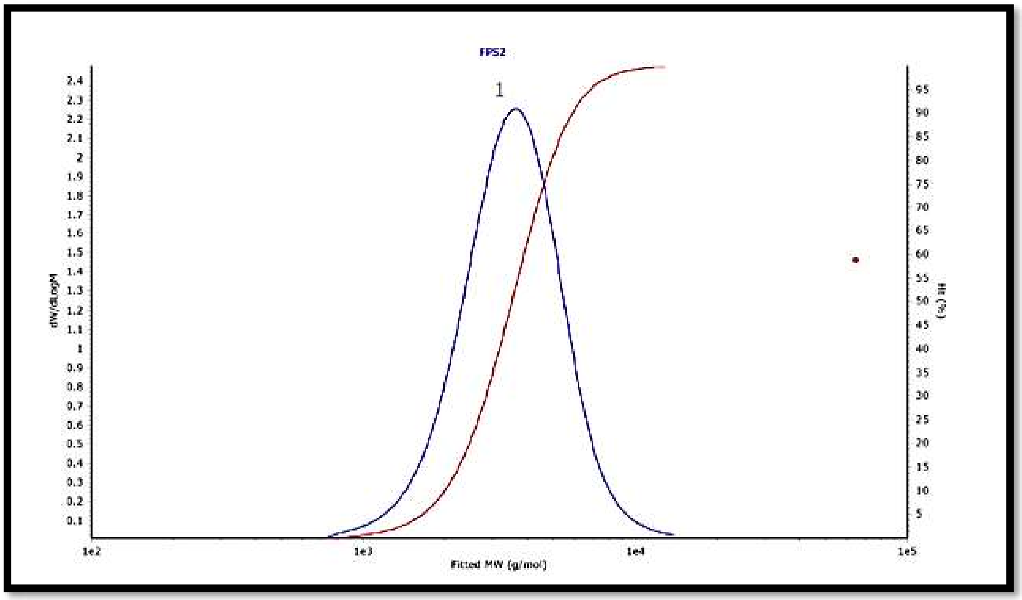

Figure 5.8. GPC chromatograph of PMMA.

GPC Analysis was carried out to know the M_n and PDI. From the above GPC analysis of Figure 5.8, M_n is 3138 g/mol. And PDI is 1.2 which indicates the narrow molecular weight distribution. The MW from theoritical and from GPC value is near to each other.

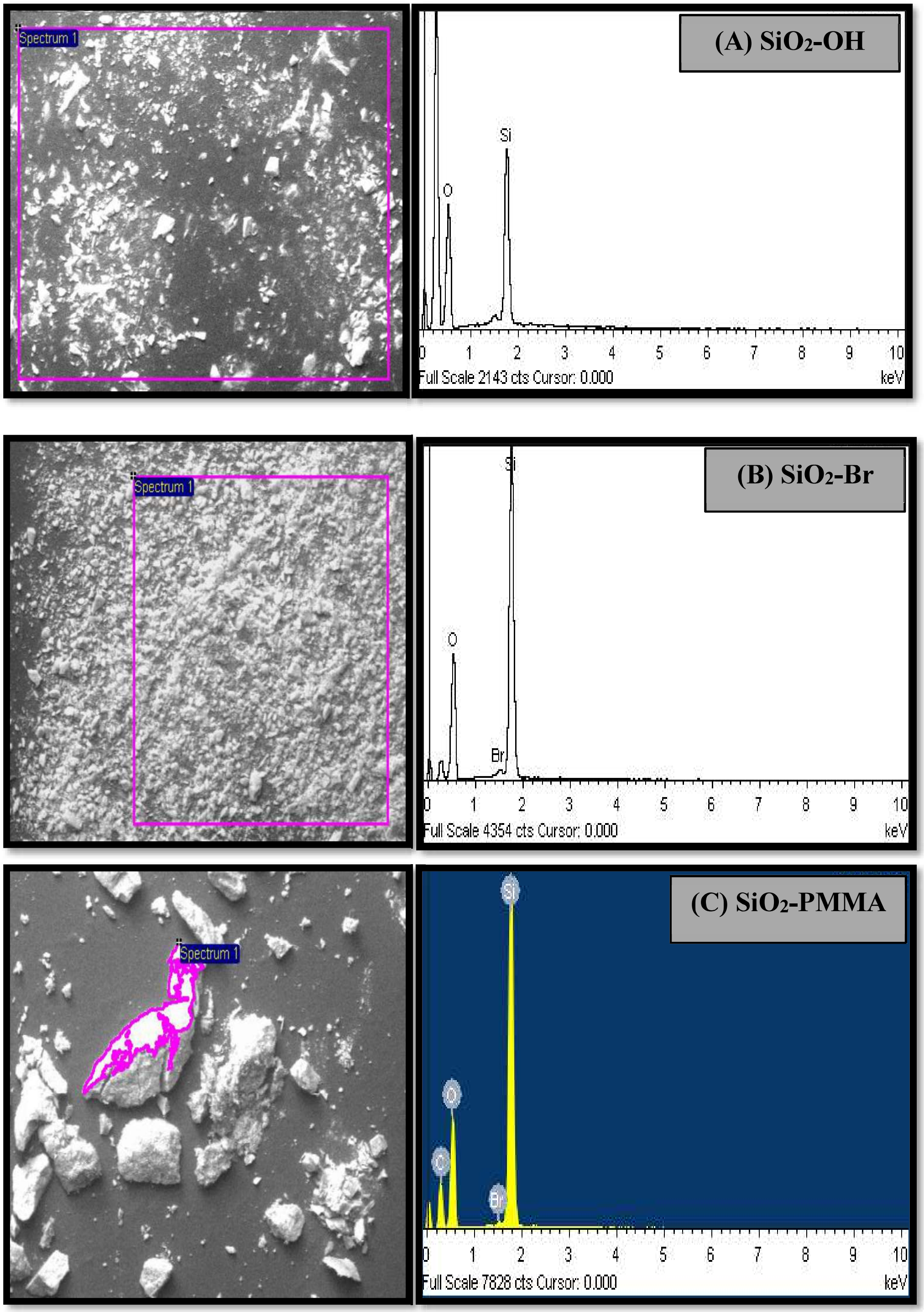

Figure 5.9. EDS Analysis of (A) SiO_2-OH (B) SiO_2-Br (C) SiO_2-g-PMMA.

In Figure 5.9, the elemental composition of the end-functionalized materials was analyzed using EDS. The EDS analysis of PMMA confirmed the successful conversion of MMA to PMMA. The EDS analysis image of SiO_2-OH confirmed the successful purification of fumed silica and complete removal of hydrocarbons. The Figure for SiO_2-Br showed that the percentage of bromine was contained 1.49%. After the polymer grafting onto the fumed silica surface and the formation of SiO_2-g-PMMA, the percentage of bromine content decreased to 0.33%. This final bromine end group polymer is known as a macroinitiator for further initiation and grafting, which can be extended up to several monomeric units.

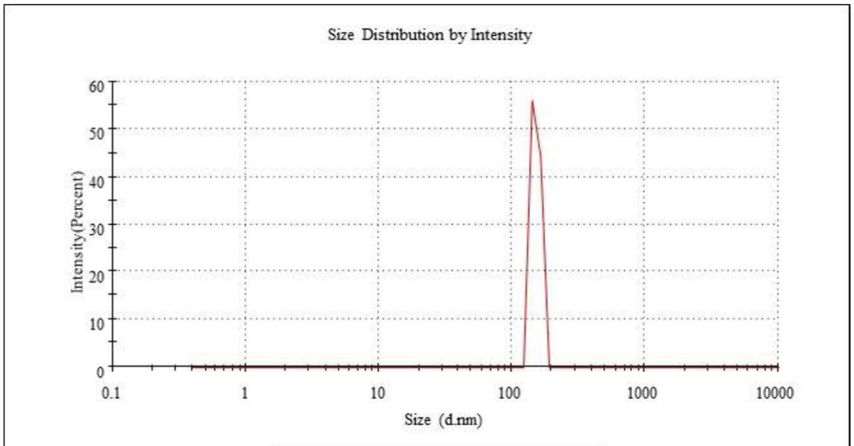

(A) SiO_2-OH (d nm): 151.7

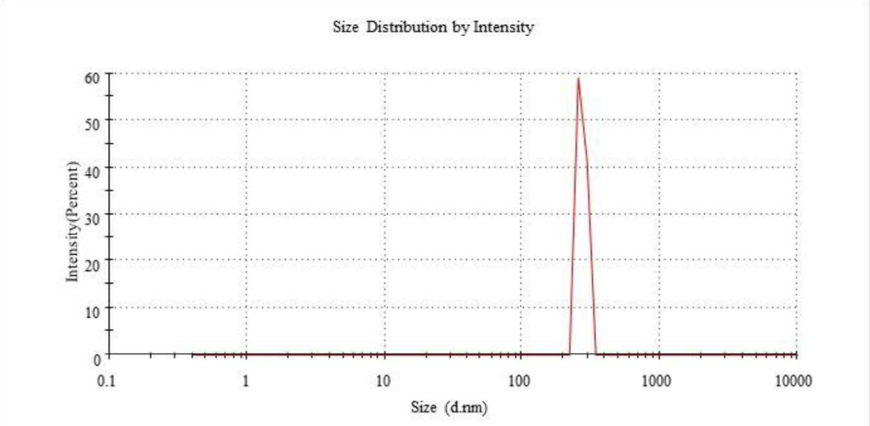

(B) SiO_2-Br (d nm): 271.6

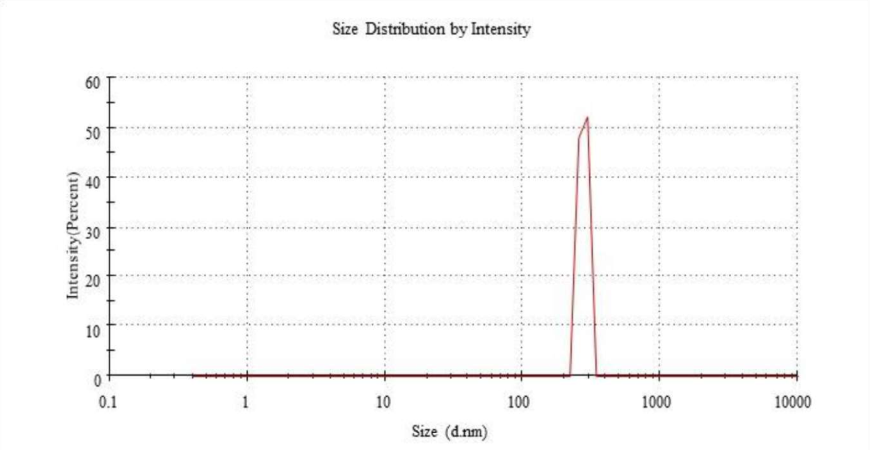

(C) SiO_2-PMMA (d nm): 276.0

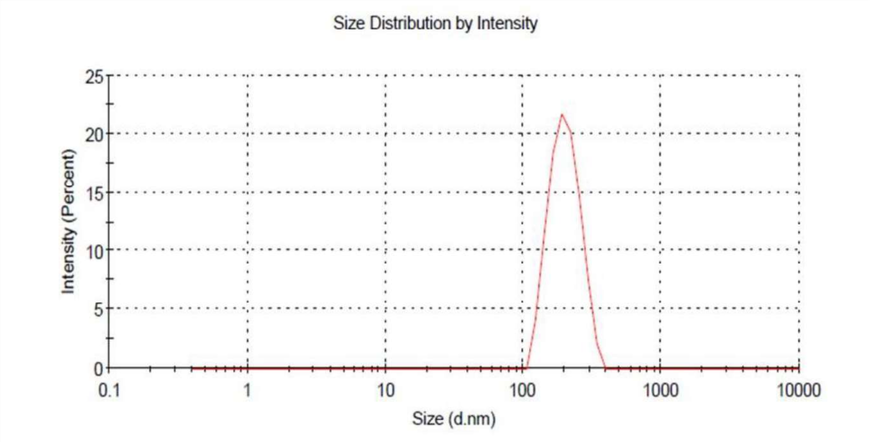

(D) SiO_2-PGMA (d nm): 257.1

Figure 5.10. DLS Analysis of (A) SiO_2-OH (B) SiO_2-Br (C) SiO_2-PMMA, and (D) SiO_2-PGMA.

Figure 5.10 explained about particle size distribution of polymer grafted silica materials. The initial particle size of purified fumed silica, as shown in Figure 5.10 (A), was found to be 151.7 nm. Following surface modification, the particle size increased to 271.6 nm, as depicted in Figure 5.10 (B). Treatment with MMA monomer further increased the particle size to 276 nm, while treatment with GMA resulted in a particle size of 257.1 nm, as shown in Figure 5.10 (C). The presence of a single peak in the size distribution profile indicates the successful surface grafting of the polymer. These findings demonstrate the effectiveness of the surface modification approach in increasing the particle size of the polymer grafted silica materials.

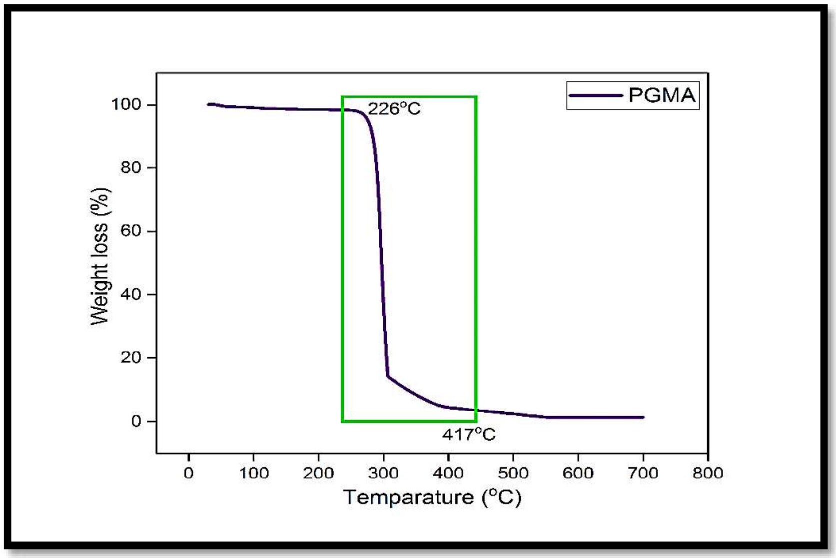

Figure 5.11. TGA analysis of SiO_2-g-PGMA.

TGA analysis was used to determine the thermal properties of SiO_2-g-PGMA. The SiO_2-g-PGMA TGA results have been shown in Figure 5.11. When heated from ambient temperature to 700 °C, SiO_2-g-PGMA has a weight loss of 94.28% at about 420 °C (degradation begins at 226 °C and ends at 417 °C). Furthermore, the percentage G is 94.3%, which was calculated using the formula described in the previous section. The calculation of %G is shown below,

$$\%G = m_{org} / m_o * 100$$

$$= 9.761mg/10.35mg * 100$$

$$= 94.3\%$$

From the TGA curve of the SiO_2-g-PMMA, the polymer grafting on the functionalized silica surface was determined. When the temperature deterioration started at 148°C and ended at 475°C, the weight loss of the final product was 8.29%. Figure 5.12 displays the thermal characteristics of SiO_2-g-PMMA. The result indicates that the %G is 6.1%.

$$\%G = m_{org} / m_o * 100$$

$$= 0.278mg / 4.525mg * 100 = 6.1\%$$

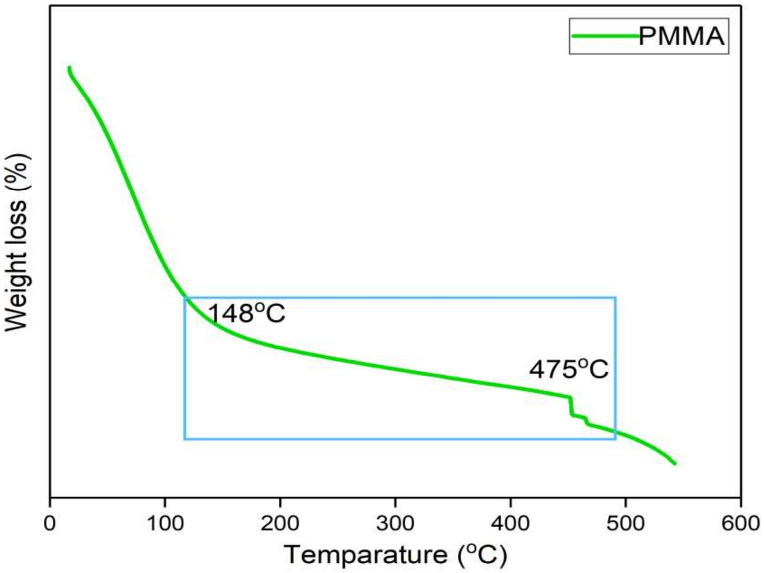

Figure 5.12. TGA Analysis of SiO_2-PMMA.

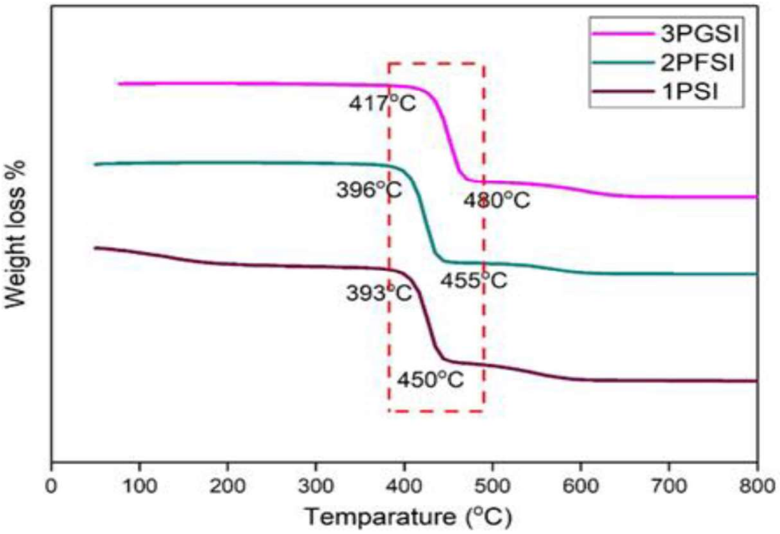

Figure 5.13. TGA analysis of (1PSI) Polymer with pristine fumed silica, (3PGSI) Polymer with functionalizes fumed silica, (2PFSI) Polymer with grafted fumed silica.

According to Figure 5.13, 1PSI represents a TGA investigation of a synthetic polymer, with pure silica starting to degrade at 393 °C. The final graph of the 3PGSI has a greater degradation temperature than the simply pristine silica, whereas the 2PFSI combines a synthetic polymer with functionalized fumed silica and has a wider temperature range. The thermal stability of the blending also increases as the percentage of polymer grafted fumed silica increases.

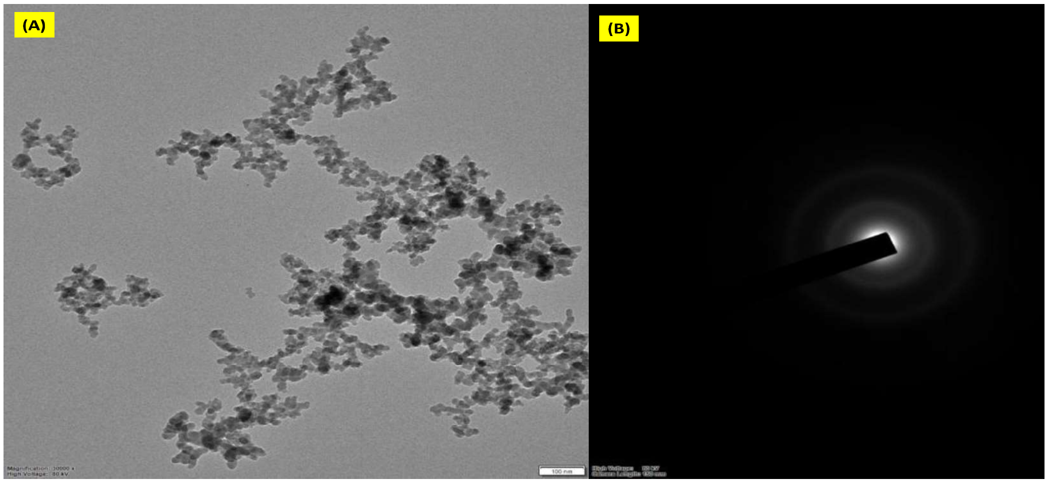

Figure 5.14. TEM Images of (A) Pristine fumed silica, (B) Diffraction pattern.

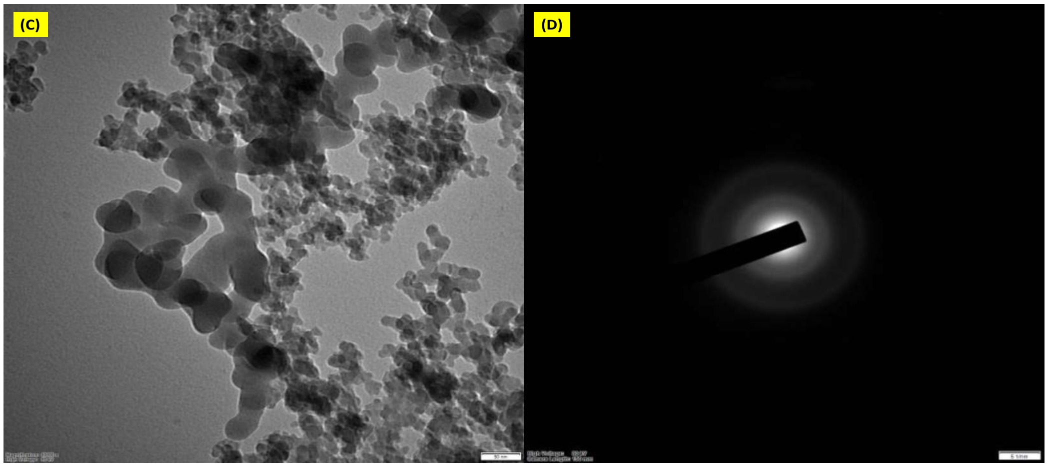

Figure 5.15. TEM Images of (C) Surface grafted fumed silica, (D) Diffraction pattern.

TEM was used to examine the morphologies of pristine silica particles and functional silica particles changed by ATRP. The silica particles are dispersed in methanol and the particle size is 100 nm in Figure 5.14 (A). The pristine silica was well separated while the grafted silica properly aggregated. When the silica coated with the polymer it became aggregation nature and roughly spherical nature of the particles observed, it shows in fig 5.15 (C) with 50 nm particle size. Figure 5.15 (B) and Figure 5.15 (D) both were the diffraction pattern of the material tested. Electron diffraction was the phenomenon resulting from the interaction between electrons and materials which was tested, producing a pattern of ring confirmed the pristine fumed silica and synthesized grafted fumed silica have amorphous nature.

5.5. Conclusions

In brief, the successful synthesis of PMMA via ATRP was confirmed by FT-IR analysis. After synthesis of PMMA it was gives idea about how the surface grafting occurred. The purification fumed silica and its functionalization was confirmed by EDS and FT-IR analysis. Furthermore, polymer grafted from fumed silica was successfully prepared by ATRP technique. After the grafting the particle size increases, which was confirmed by DLS. The aggregation of the grafted silica particles observed via TEM. The percentage grafting (%) G of the final material and % weight loss of the ATRP reaction is confirmed by the TGA analysis. The polymer grafted silica material will be further used as a filler in the next to the polymer.

5.6. References

[1] Barthel, H.; Rösch, L.; Weis, J. Fumed Silica - Production, Properties, and Applications. In *Organosilicon Chemistry II: From Molecules to Materials*; 1996. https://doi.org/10.1002/9783527619894.ch91.

[2] Barthel, H.; Rösch, L.; Weis, J. Fumed Silica - Production, Properties, and Applications. In *Organosilicon Chemistry Set: From Molecules to Materials*; 2005. https://doi.org/10.1002/9783527620777.ch91a.

[3] Avnir, D.; Farin, D.; Pfeifer, P. Surface Geometric Irregularity of Particulate Materials: The Fractal Approach. *J Colloid Interface Sci*, **1985**, *103* (1). https://doi.org/10.1016/0021-9797(85)90082-7.

[4] Škvarla, J.; Škvarla, J. A Swellable Polyelectrolyte Gel-like Layer on the Surface of Hydrous Metal Oxides in Simple Electrolyte Solutions: Hematite vs. Silica Colloids. *Colloids and Surfaces A: Physicochemical and Engineering Aspects*. 2017. https://doi.org/10.1016/j.colsurfa.2016.11.018.

[5] Penelas, M. J.; Contreras, C. B.; Giussi, J. M.; Wolosiuk, A.; Azzaroni, O.; Soler Illia, G. J. A. A. Controlling Dispersion, Stability and Polymer Content on PDEGMA-Functionalized Core-Brush Silica Colloids. *Colloids Surf A Physicochem Eng Asp*, **2019**, *574*. https://doi.org/10.1016/j.colsurfa.2019.04.035.

[6] Wang, Z.; Fantin, M.; Sobieski, J.; Wang, Z.; Yan, J.; Lee, J.; Liu, T.; Li, S.; Olszewski, M.; Bockstaller, M. R.; et al. Pushing the Limit: Synthesis of SiO2- g-PMMA/PS Particle Brushes via ATRP with Very Low Concentration of Functionalized SiO2-Br Nanoparticles. *Macromolecules*, **2019**, *52* (22). https://doi.org/10.1021/acs.macromol.9b01973.

[7] Pyun, J.; Matyjaszewski, K. Synthesis of Nanocomposite Organic/Inorganic Hybrid Materials Using Controlled/"living" Radical Polymerization. *Chemistry of Materials*. 2001, pp 3436–3448. https://doi.org/10.1021/cm011065j.

[8] Karkare, P.; Kumar, S.; Murthy, C. N. ARGET-ATRP Using β-CD as Reducing Agent for the Synthesis of PMMA-b-PS-b-PMMA Triblock Copolymers. *J Appl Polym Sci*, **2019**. https://doi.org/10.1002/app.47117.

[9] Kumar, S.; Lee, J. S.; Murthy, C. N. Synthesis and Characterization of BAB and CBABC Tri- and PentaBlock Copolymers via Atom Transfer Radical Polymerization.

Macromol Res, **2011**. https://doi.org/10.1007/s13233-011-1012-8.

[10] Wu, T.; Zhang, Y.; Wang, X.; Liu, S. Fabrication of Hybrid Silica Nanoparticles Densely Grafted with Thermoresponsive Poly(N-Isopropylacrylamide) Brushes of Controlled Thickness via Surface-Initiated Atom Transfer Radical Polymerization. *Chemistry of Materials*, **2008**, *20* (1), 101–109. https://doi.org/10.1021/cm702073f.

[11] Lee, S. B.; Koepsel, R. R.; Morley, S. W.; Matyjaszewski, K.; Sun, Y.; Russell, A. J. Permanent, Nonleaching Antibacterial Surfaces, 1. Synthesis by Atom Transfer Radical Polymerization. *Biomacromolecules*, **2004**, *5* (3), 877–882. https://doi.org/10.1021/bm034352k.

[12] Liu, Y.; Wang, X.; Song, W.; Wang, G. Synthesis and Characterization of Silica Nanoparticles Functionalized with Multiple TEMPO Groups and Investigation on Their Oxidation Activity. *Polym Chem*, **2015**, *6* (43), 7514–7523. https://doi.org/10.1039/c5py01190f.

[13] Chen, J.; Xiang, J.; Cai, Z.; Yong, H.; Wang, H.; Zhang, L.; Luo, W.; Min, H. Synthesis of Hydrophobic Polymer Brushes on Silica Nanoparticles via the Combination of Surface-Initiated ATRP, ROP and Click Chemistry. *Journal of Macromolecular Science, Part A: Pure and Applied Chemistry*, **2010**, *47* (7). https://doi.org/10.1080/10601325.2010.483357.

[14] Penelas, M. J.; Contreras, C. B.; Giussi, J. M.; Wolosiuk, A.; Azzaroni, O.; Soler Illia, G. J. A. A. Controlling Dispersion, Stability and Polymer Content on PDEGMA-Functionalized Core-Brush Silica Colloids. *Colloids Surf A Physicochem Eng Asp*, **2019**, *574*, 12–20. https://doi.org/10.1016/j.colsurfa.2019.04.035.

[15] Zhang, J.; Jiang, L.; Pan, K.; Yi, Z.; Dan, Y. Controlled Polymerization of Methylmethacrylate from Fumed SiO2 Nanoparticles through Atom Transfer Radical Polymerization. *Polym Int*, **2014**, *63* (3), 413–419. https://doi.org/10.1002/pi.4514.

[16] Wang, X.; Jing, S.; Liu, Y.; Qiu, X.; Tan, Y. Preparation of Dithiocarbamate Polymer Brush Grafted Nanocomposites for Rapid and Enhanced Capture of Heavy Metal Ions. *RSC Adv*, **2017**, *7* (22). https://doi.org/10.1039/c6ra28890a.

[17] Kubiak, J. M.; Macfarlane, R. J. Forming Covalent Crosslinks between Polymer-Grafted Nanoparticles as a Route to Highly Filled and Mechanically Robust Nanocomposites. *Adv Funct Mater*, **2019**, *29* (44). https://doi.org/10.1002/adfm.201905168.